PHYSICAL REVIEW A **68**, 041401(R) (2003)

Two-dimensional momentum imaging of Rydberg states using half-cycle pulse ionization and velocity map imaging

A. Wetzels,[1] A. Gürtler,[1] F. Roşca-Prună,[1] S. Zamith,[1] M. J. J. Vrakking,[1] F. Robicheaux,[2] and W. J. van der Zande[1,3]
[1]*FOM Institute for Atomic and Molecular Physics, Kruislaan 407, 1098 SJ Amsterdam, The Netherlands*
[2]*Department of Physics, Auburn University, Auburn, Alabama 36849, USA*
[3]*Department of Molecule and Laser Physics, University of Nijmegen, Nijmegen, The Netherlands*
(Received 28 March 2003; published 13 October 2003)

The influence of the half-cycle pulse (HCP) kick on the asymptotic velocity of the ejected electron has been studied for excited xenon atoms ($n^*=34$) in the presence of a static electric field (220 V cm^{-1}). We find that the HCP does not change the momentum distribution perpendicular to the kick direction. Therefore half-cycle pulse ionization and electron velocity map imaging can be used to obtain two-dimensional momentum distributions of atomic Rydberg states. Semiclassical and quantum mechanical calculations complement the experimental results.

DOI: 10.1103/PhysRevA.68.041401 PACS number(s): 32.60.+i, 32.80.−t, 32.10.−f, 34.60.+z

Since the beginning of quantum mechanics, matter is described in terms of its wave function. Observable quantities are evaluated as expectation values of associated Hermitian operators. Details of the wave function remain mostly hidden. In $(e,2e)$ experiments [1], the wave function of an atom or molecule in its ground state is retrieved in momentum space using the fact that at sufficiently high energy ($\sim$1 keV) the electron-electron collision is impulsive. From the final momentum and energy of both electrons (measured in coincidence) the binding energy of the ejected electron as well as its momentum at the moment of the collision can be retrieved. Two conditions determine the success of the $(e,2e)$ method. The ionization cross section does not depend on the actual momentum of the electron. In the second condition the collision is sudden with respect to the classical motion of the electrons in the atom. These two conditions can be considered as general requisites for direct methods that measure details of a wave function.

Electromagnetic radiation is an attractive alternative for fast electrons. Here, we present the use of ultrafast, subpicosecond half-cycle pulses (HCP) with a short duration compared to the classical roundtrip time of the Rydberg electrons. In the short pulse limit, the interaction of the HCP with the Rydberg electron is described as a momentum kick:

$$\Delta\mathbf{p} = -\int \mathbf{E}_{HCP}(t)dt, \tag{1}$$

where $\mathbf{E}_{HCP}(t)$ is the electric field of the HCP [2]. The resulting energy transfer is given by

$$\Delta E = \mathbf{p}_0 \cdot \Delta\mathbf{p} + \tfrac{1}{2}\Delta p^2, \tag{2}$$

where $\mathbf{p}_0$ is the momentum of the electron at the moment of the HCP interaction. In practice, we achieve near 100% ionization of a sample of Rydberg atoms with one single HCP. Hence, the ionization probability does not depend on the actual momentum of the ionized electron in its orbit.

The method proposed in this paper builds on the fact that a kick does not change the component of the momentum in the directions perpendicular to the kick. An illustration of the experimental principle is given in Fig. 1. In this article, the kick direction implies the direction of the force felt by the electron.

This new concept differs and complements the method presented by Jones [3], who used HCP ionization to determine the momentum distribution in one dimension along the kick direction. Robicheaux [4] treated this process theoretically. In their method, the increase in ionization, yield as a function of the kick strength, is equal to the probability of finding an electron with a momentum component $\mathbf{p}_0$ in the direction of the kick. The method requires a scan over different HCP strengths. In contrast, the present method uses only one strong HCP setting. Moreover, the 2D momentum maps are obtained directly without taking the derivative of experimental data.

First, we show that HCP ionization provides two-dimensional momentum information by comparing experimental momentum images, which are obtained under different experimental conditions. Second, classical calculations of the HCP ionization process are used to support the validity of

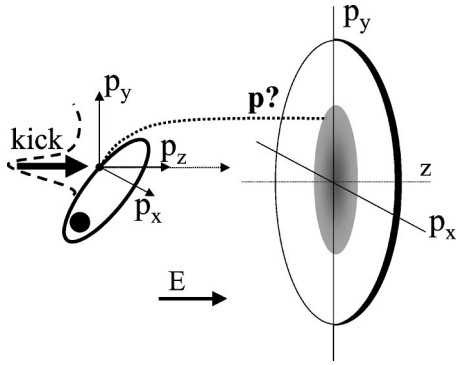

FIG. 1. Illustration of the experimental principle. A Rydberg atom is ionized with a HCP, here polarized in the *z* direction. The HCP only changes the momentum component of the electron along the *z* axis (dashed arrow), not the *x*, *y* components. Using velocity map imaging the electron is imaged onto a detector in such a way that the distance of the electron from the center is directly proportional to the momentum component in the *xy* plane. The *z* direction remains undetected.

the momentum mapping of a Rydberg state.

In our experiment, xenon atoms were prepared in the $^3P_{J=2}$ ($5p^5 6s$) metastable state in an electron impact source [5] and expanded into a molecular beam. Rydberg atoms were created in a static electric field of 220 V/cm using one-photon excitation with light from a nanosecond dye laser. The states just below the saddle point were excited with effective principal quantum number $n^*=34$. The electron roundtrip time in these states, $\tau_K=6$ ps, is longer than the HCP (width 0.5–1 ps). We distinguish two dye laser polarization directions, parallel (along the *z* axis) and perpendicular (along the *x* axis) to the electric field, forming Rydberg states with magnetic quantum number $m=0$ and $m=\pm 1$, respectively. The static electric field was strong enough to reach the *n*-mixing regime. Due to the bandwidth ($0.2\ \mathrm{cm}^{-1}$) and duration of the laser pulse (8 ns), an incoherent sum of *k* states, eigenstates in a static electric field, was formed. About 500 ns later, the highly excited Rydberg states were subjected to a strong HCP. The HCP was generated by illuminating a voltage biased GaAs wafer with a 100 fs laser pulse from a Ti:Sapphire laser [6,7]. The polarization of the HCP was either perpendicular (*x* direction) or (anti)parallel (*z* direction) to the static electric field. The dye laser and HCP counterpropagate along the *y* axis. The velocity components perpendicular to the kick directions were measured. In an earlier paper we showed that the asymptotic momentum component parallel to the kick is much smaller than the momentum after the HCP due to the influence of a weak ''tail,'' with opposite polarity following the main HCP peak [8].

The final velocity and angular distributions of the electrons were measured by velocity map imaging [9]. In this technique, the position of the electrons on the detector only depends on the asymptotic *x* component and *y* component of the velocity of the electrons. The instrument's design includes an ion optical lens, which removes the sensitivity of the detected position to the starting position of the electron. Inside the time-of-flight tube an extra Einzel lens is present [10], which linearly magnifies the momentum maps onto a microchannel plate detector (MCP). A charge-coupled device (CCD) camera is used to record the image from the phosphor screen behind the MCP. The velocity scale in the *x* direction and *y* direction of the images was calibrated independently. The momentum scale in the images is derived from near threshold photo-ionization by Nicole *et al.* [11], where analytical calculations provide the relation between the displacement $\Delta x, \Delta y$ of the photoionized electrons on the detector and their asymptotic momentum p_x, p_y [12].

Figure 2 shows two raw images taken at two different kick strengths parallel (in the *z*-direction) to the electric field, a weak kick ($\Delta p=3\times 10^{-3}$ a.u.) giving about 10% ionization and a strong kick ($\Delta p=6\times 10^{-2}$ a.u.) giving nearly 100% ionization. The dye laser was polarized perpendicular to the electric field, exciting $m=\pm 1$ Rydberg states. The momentum distribution broadens upon an increase of the HCP field strength and ionization yield. The images are cylindrically symmetric as will be explained below. At low kick strength only the electrons with high momentum in the kick direction (*z* direction), and therefore correspondingly low

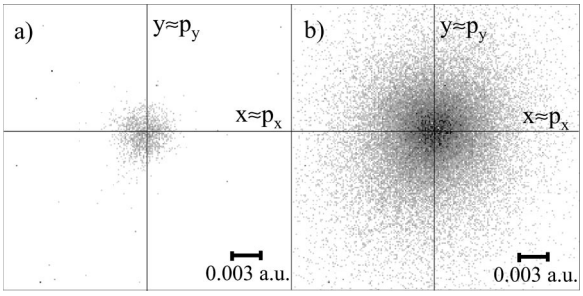

FIG. 2. Raw images taken at two different HCP kick strengths, (a) 10% ionization, (b) 100% ionization using parallel kick. The momentum scale is indicated in the figure.

momentum in the directions perpendicular to the kick (*x* direction and *y* direction), can ionize. The final momentum distribution is influenced by the focussing effect of the combined Coulomb potential and external static electric field. We will show that at high kick strengths, where the strength of the HCP suffices that 100% of the excited Rydberg state population is being ionized, we measure the momentum distribution of the initial Rydberg state. At these high kick strengths, the kinetic energy of the electron after the HCP kick is significantly larger than 10 meV. It has been shown in simulations of photoionization experiments [12] that at this kinetic energy the influence of the Coulomb force is negligible, in spite of the small measured p_x and p_y values.

The kick does not change the component of the momentum in the directions perpendicular to the kick. An empirical method for estimating the influence of the HCP on the directions perpendicular to the kick is to compare the momentum distributions in the *x* and *y* direction when kicking in the *z* direction with the momentum distribution in the *y* direction upon kicking in the *x* direction. In all of these cases the observed distributions should closely resemble each other as the same momentum distribution is being imaged. Figure 3(a) shows this comparison for an $m=0$ Rydberg state and in Fig. 3(b) for an $m=\pm 1$ Rydberg state in the form of projected one-dimensional momentum distributions directly derived from the raw images. The measured momentum distributions in both Figs. 3(a) and 3(b) are similar, while the momentum distribution of the $m=0$ Rydberg state is clearly narrower than the one for the $m=\pm 1$ Rydberg state. *A priori*, the difference in initial preparation ($m=0$ versus $m=\pm 1$) with the dye laser was expected to be very small. The nanosecond dye laser prepared an incoherent superposition of many *k* states. Each of these *k* states is a superposition of many different *l* states (up to $l=33$). For these high *l* states a difference of one unit in the magnetic quantum number is expected to be insignificant. The increase in width of the $m=\pm 1$ momentum distribution is the influence of the centrifugal barrier in the potential keeping the electrons away from the *z* axis. The superposition of many *k* states results in the disappearance of the nodal structure, often associated with a wave function.

The initial momentum distributions of the Rydberg state and the expected velocity map images after HCP ionization were calculated using trajectory calculations and quantum mechanical calculations. The classical calculations were per-

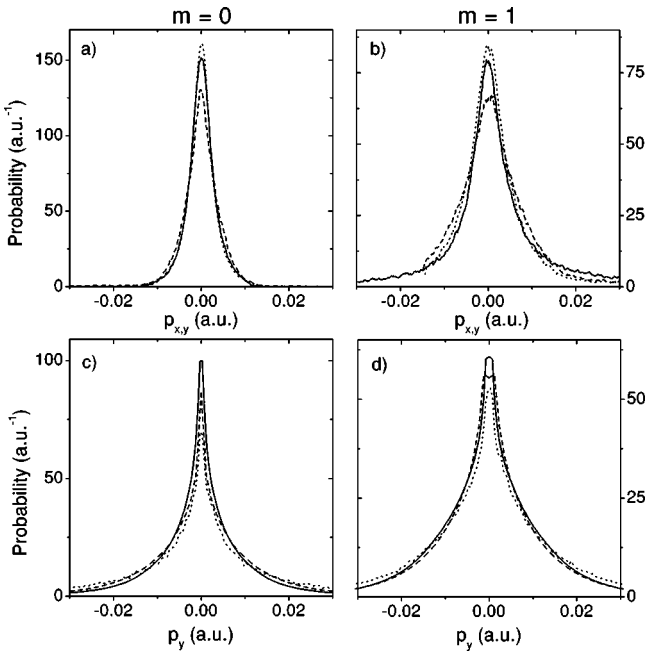

FIG. 3. Measured and calculated one-dimensional momentum distributions. (a),(b) Measured momentum distributions in the x and y directions for a HCP polarized in the z direction (black line and dotted line) and measured momentum distribution in the y direction for a HCP polarized in the x direction (dashed line). (c),(d) Calculated momentum distribution in the y direction before and after a HCP kick. (black line) Initial momentum distribution using trajectory calculations. Initial momentum distribution using quantum calculations (dashed line). Distribution using HCP polarization along the z direction (dotted line). The distribution using HCP polarization along the x direction follows the calculated momentum distributions even more closely and is not shown.

formed by solving the three-dimensional classical equations of motion for a hydrogenic electron in an electric field using a fourth-order Runge-Kutta algorithm. A realization of quantum states using classical trajectories is not unambiguous. The initial state is a stationary Rydberg state given by the principal quantum number $n=34$. The dye laser excites the p character in the Stark state. As mentioned, the orbital angular momentum l is no longer a conserved quantity in the static electric field, but in classical terms l oscillates. The polarization of the dye laser sets the magnetic quantum number, $m=0$ or $m=\pm 1$. Also metastable xenon has an ionic core with $J=3/2$. The interaction with the many-electron core causes a precession of the long axis of the elliptic orbit when the electron penetrates the core while conserving angular momentum and its projection on the quantization axis. With the laser polarization along the x axis, the initial directionality along the x axis disappears as a consequence of this precession and the long 500 ns delay of the HCP pulse. Cylindrical symmetry is restored around the z axis. In our classical trajectories, l_z takes random values in certain intervals, $l_z \in [-0.5,0.5]$ for $m=0$ and $l_z \in [-1.5,-0.5],[0.5,1.5]$ for $m=\pm 1$ respectively. In the trajectories, we follow the electron during one complete l oscillation starting at $l=1$. The HCP pulse (FWHM 1 ps, $\mathbf{E}_{\max}$ 8 kV/cm) starts randomly during one l oscillation. The velocity distribution of the electron in the x,y directions far away from the core, where the Coulomb field is negligible, represents the velocity map. The quantum mechanical calculations reproduce the momentum distribution of the excited Rydberg state by adding the momentum distributions of all 34 hydrogenic k states for $n=34$ as a model of the n-mixing regime.

The initial one-dimensional momentum distribution perpendicular to the electric field axis, calculated both classical and quantum mechanical, is plotted in Figs. 3(c) and 3(d) together with the classically calculated momentum distributions involving the HCP in the z direction. The quantum mechanical calculations of the initial distribution agree very well with the classical calculations, supporting the usefulness of the latter calculations. The distributions after the HCP kick depend very little on the direction of the kick. The distribution in the x direction resembles the calculated initial momentum distributions even more closely than the shown distribution in the z direction. These results corroborate that HCP kick hardly changes the momentum components perpendicular to the kick direction. The calculations reproduce the magnitude of the observed momentum values and support the observation that the momentum distribution of the $m=0$ Rydberg state is narrower than the momentum distribution of the $m=\pm 1$ Rydberg state. If the Coulomb force would affect the momentum distributions because of the long-range character of this interaction, this would show up in these calculations. One small distortion is observed in the classical calculations for the case of kicks in the z direction [Figs. 3(c) and 3(d)]. The trajectory calculations indicate that electrons present on the z axis at the moment of the kick are accelerated towards the ionic core resulting in large angular scattering, which adds signal at large momentum values. This phenomenon is not observed in the measurements shown in Figs. 3(a) and 3(b) reflecting that this strong Coulomb scattering may be a product of the trajectory calculations involving a point charge. Both experimental data and calculations show that the fact that the interaction is not perfectly sudden (1 ps of the HCP in the calculation versus 6 ps electron orbit time) does not influence the momentum distribution.

A comparison of the computational and experimental results reveals that the measured momentum distribution is narrower and less peaked than the calculated momentum distribution. The resolution of the velocity map imaging technique at small kick strengths equals about 0.001 a.u., sufficient to detect the sharp calculated distributions. We note that the most important differences between our observations and the calculated results are in the wings of the distributions. This difference cannot be explained by a finite resolution. All computational results are performed for hydrogen. We stress that the calculations for xenon with its complex core are highly nontrivial. Two effects may be important, the angular momentum of the core and the presence of the core electrons. The initial state, which consists of different k states from different values of n, can not be reproduced easily. In the calculations, all k-states for one n value are used. These effects may well explain the small differences.

The requirement of 100% ionization and an interaction time that is short with respect to the radial orbiting time sets

the limitations of this method at present. Only states near the saddle point can be fully ionized. The minimum value of $n = 25$. Wesdorp *et al.* [13] showed that when $n > 70$ the ionization is surpressed by the influence of the tail of the HCP. This sets an upper limit to n. The present experiment requires a static electric field. Although velocity map imaging has been done for the fragment ions of molecular fragmentation created in field free conditions using delayed pulsed field extraction by Gebhardt *et al.* [14], this technique cannot yet be applied for the much faster electrons. Zobay and Alber have treated aspects of the field-free case theoretically [15]. The study of lower lying states using HCP excitation requires shorter half-cycle pulses. Recent developments in the generation of very few-cycle radiation [16] with a few femtosecond duration may open the possibility for the study of lower lying Rydberg states. In future the use of atomic hydrogen would make it possible to break the cylindrical symmetry which is found in the xenon case. The advantage of the study of laser generated Rydberg states is the possibility to image time dependent wave functions in a pump-probe experiment using a subpicosecond laser pulse in combination with the subpicosecond HCP as has been achieved by Jones and coworkers for the one-dimensional momentum distribution [3].

In summary, the advent of ultrafast HCP in combination with the imaging technique produces directly two-dimensional momentum wave function maps. Consistency is found when comparing different measurement geometries and when comparing the calculated initial momentum distributions with the calculated velocity map images. The system used in the present experiment showed a large amount of symmetry because of the presence of core scattering associated with the complex nature of the xenon core.

We would like to thank H.G. Muller, L.D. Noordam, and S. Woutersen for their comments. We thank A. Buyserd, E. Springate, and S.Asseev for providing the femtosecond laser. We acknowledge the EU-Network Cocomo, Grant No. HPRNT-CT-1999-00129. This work is part of the research program of the ''Stichting voor Fundamenteel Onderzoek der Materie (FOM),'' which is financially supported by the ''Nederlandse Organisatie voor Wetenschappelijk Onderzoek (NWO).'' F. Robicheaux was supported by the National Science Foundation.

[1] E. Weigold, S.T. Hood, and P.J.O. Teubner, Phys. Rev. Lett. **30**, 475 (1973); S.T. Hood, I.E. McCarthy, P.J.O. Teubner, and E. Weigold, Phys. Rev. A **8**, 2494 (1973).

[2] R.R. Jones, D. You, and P.H. Bucksbaum, Phys. Rev. Lett. **70**, 1236 (1993); C.O. Reinhold, M. Melles, H. Shao, and J. Burgdörfer, J. Phys. B **26**, L659 (1993); C.O. Reinhold, J. Burgdörfer, R.R. Jones, C. Raman, and P.H. Bucksbaum, *ibid.* **28**, L457 (1995); M.T. Frey, F.B. Dunning, C.O. Reinhold, and J. Burgdörfer, Phys. Rev. A **53**, R2929 (1996).

[3] R.R. Jones, Phys. Rev. Lett. **76**, 3927 (1996); M.B. Campbell, T.J. Bensky, and R.R. Jones, Phys. Rev. A **58**, 514 (1998).

[4] F. Robicheaux, Phys. Rev. A **56**, R3358 (1997).

[5] A. Kohlhase and S. Kita, Rev. Sci. Instrum. **57**, 2925 (1986).

[6] B.B. Hu, J.T. Darrow, X.-C. Zhang, and D.H. Auston, Appl. Phys. Lett. **56**, 886 (1990); B.B. Hu, X.-C. Zhang, and D.H. Auston, Phys. Rev. Lett. **67**, 2709 (1991); D. You, R.R. Jones, and P.H. Bucksbaum, Opt. Lett. **18**, 290 (1993).

[7] A. Wetzels, A. Gürtler, A. Buijserd, T. Vijftigschild, H. ter Horst, and W.J. van der Zande, Rev. Sci. Instrum. **74**, 3180 (2003).

[8] A. Wetzels, A. Gürtler, L.D. Noordam, F. Robicheaux, C. Dinu, H.G. Muller, M. Vrakking, and W.J. van der Zande, Phys. Rev. Lett. **89**, 273003 (2002).

[9] A.T.J. Eppink and D.H. Parker, Rev. Sci. Instrum. **68**, 3477 (1997).

[10] H.L. Offerhaus, C. Nicole, F. Lépine, C. Bordas, F. Roşca-Prună, and M.J.J. Vrakking, Rev. Sci. Instrum. **72**, 3245 (2001).

[11] C. Nicole, I. Sluimer, F. Roşca-Prună, M. Warntjes, M. Vrakking, C. Bordas, F. Texier, and F. Robicheaux, Phys. Rev. Lett. **85**, 4024 (2000); C. Nicole, H.L. Offerhaus, M.J.J. Vrakking, F. Lepine, and C. Bordas, *ibid.* **88**, 133001 (2002).

[12] C. Bordas, Phys. Rev. A **58**, 400 (1998).

[13] C. Wesdorp, F. Robicheaux, and L.D. Noordam, Phys. Rev. Lett. **87**, 083001 (2001).

[14] C.R. Gebhardt, T.P. Rakitzis, P.C. Samartzis, V. Ladopoulos, and T.N. Kitsopoulos, Rev. Sci. Instrum. **72**, 3848 (2001).

[15] O. Zobay and G. Alber, Phys. Rev. A **60**, 1314 (1999).

[16] A. Baltuska, T. Udem, M. Uiberacker, M. Hentschel, E. Goulielmakis, C. Gohle, R. Holzwarth, V.S. Yakoviev, A. Scrinzi, T.W. Hänsch, and F. Krausz, Nature (London) **421**, 611 (2003).